

Vincent Fleischhauer*, Nora Ruprecht, and Sebastian Zaunseder

Camera-based spatial assessment of perfusion upon stimuli

<https://doi.org/10.1515/cdbme-2019-0027>

Abstract: Imaging photoplethysmography allows to capture spatio-temporal patterns related to the perfusion. One such approach is based on the analysis of the time delay between pulse waves at different locations by so-called phase maps. There are different ways to establish such maps. However, neither a comparison between existing methods has been published nor has the impact of different stimuli been sufficiently examined until today. In this work, we compare three previously published approaches for the generation of phase maps and investigate the impact of two physiological stimuli on such maps. Our results show pairwise correlation coefficients between the different approaches of phase map generation from $r = 0.65$ to $r = 0.82$, indicating substantial differences between maps. The different maps reflect our physiological expectation in varying degrees. Particularly for a weaker (distant) stimulation refinements are needed to reveal characteristic changes.

Keywords: imaging photoplethysmography, camera, cardiovascular, perfusion, phase maps

1 Introduction

Photoplethysmography (PPG) is a clinically widely used non-invasive optical method to capture blood volume changes. A contactless variation of this technique is called imaging photoplethysmography (iPPG). iPPG and PPG, both exploit variations in light modulation due to cardiovascular activity [16]. Most works on iPPG concentrate on obtaining one-dimensional signals from videos and extracting heart rate and heart rate variability (HRV). Beyond such analyses, iPPG allows spatial analyses of blood volume changes by means of so-called perfusion maps. There are several approaches to obtain perfusion maps from iPPG recordings whereby amplitude and phase maps can be extracted. Amplitude maps assess the strength and phase maps assess the temporal spread of the per-

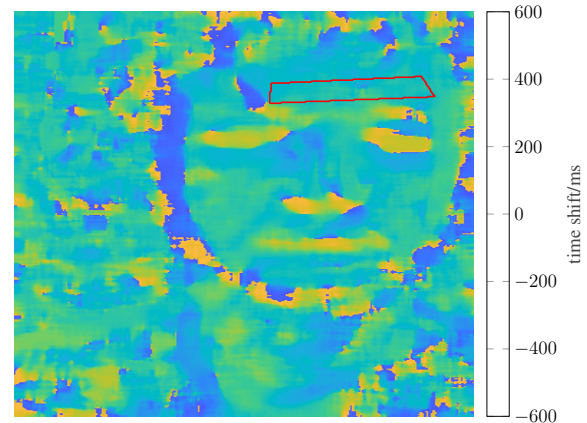


Fig. 1: Exemplary phase map of a subject of the CPT study, that was obtained by using the method of Zaunseder *et al.* [16]. The ROI is marked with a red line.

fusion (see Fig. 1). Only few works examine the generation of phase maps and their potential uses or the impact of various stimuli on them [2, 5–7, 9–12, 14–16]. To the best of our knowledge, there are no comparisons between existing methods for the generation of phase maps. This work provides a comparative validation of selected methods for the generation of phase maps during different stimuli.

2 Methods and materials

2.1 Data

The data originates from two studies, a cold face test (CFT) and a cold pressure test (CPT). In both studies a RGB camera (UI-3370CP-C-HQ, IDS) with a color depth of 12 bit, a frame rate of 100 fps and a resolution of 420×320 pixels was used for video recordings of the face. The experimental setup was illuminated by ambient and a fluorescent ceiling light. In both studies the ECG was recorded as reference data. [16] gives a comprehensive overview about the data.

Cold face test study: At the beginning, three baseline measurements were carried out. After 390 s, three subsequent CFTs were conducted. During each CFT we set two analysis intervals (before and after application of the cold stimulus), each one lasting 10 s. 21 healthy subjects (age 26.2 ± 6.69 years, 6 female) took part in the CFT study. Due to technical

*Corresponding author: Vincent Fleischhauer, Fachhochschule Dortmund, Sonnenstraße 96, Dortmund, Germany, e-mail: vincent.fleischhauer@fh-dortmund.de

Nora Ruprecht, Otto Bock Healthcare Products GmbH, Vienna, Austria

Sebastian Zaunseder, Fachhochschule Dortmund, Dortmund, Germany

problems, only 15 data sets could be analysed.

Cold pressure test study: As in the CFT study, at the beginning, three baseline measurements were carried out. We analyzed only the third baseline interval. After 480 s, the CPT started. The stimulus lasted up to three minutes. The participants were free to quit stimulation earlier. Two more analysis intervals were defined as the time interval 10 s after the start of the stimulation and as the time instant at which the systolic blood pressure reached its peak value. Like in the CFT study, the analysis intervals lasted 10 s. 22 healthy subjects (age 25.5 ± 3.73 years, 10 female) participated in the study twice, one time in supine position and one time sitting. In consequence of varying recording positions and their temporal separation, different recordings of the same subject were considered independent. One recording had to be discarded due to technical problems. Of the remaining 43 recordings, another 20 were sorted out because the respective subjects were moving too much, thereby altering the region of interest (ROI). Thus, 23 were analyzed.

2.2 Implementation

In our analyses, we only used the green channel of the video recordings as it provides the highest signal quality [13]. We spatially smoothed each frame by an averaging filter of 15×15 pixels. Furthermore, the pixel traces of the spatially smoothed video recordings were bandpass filtered by a fifth order Butterworth filter (cutoff frequencies 0.5 Hz and 6 Hz). In order to minimize sources of error, we extracted the heart rate from the reference ECG. The algorithms for phase map generation were applied to manually defined ROI on the forehead of the subjects, thus reducing ballistocardiographic effects that can arise from edges and inhomogeneities [16].

2.2.1 Methods for generation of phase maps

As of today, there are two essential approaches for the generation of phase maps from iPPG recordings. One approach uses synchronous detection [5] and the other one uses cross-correlation [2]. Both approaches need a reference function that represents the pulsation of the heart in order to estimate local phase delays of the perfusion. For our comparison, we implemented three different methods for the generation of phase maps, covering both essential approaches with different reference functions.

Method 1: The first method to yield phase maps based on synchronous detection was proposed by Kamshilin *et al.* [5]. Synchronous detection is a coherent demodulation method, which is used in communication systems to synchronously demod-

ulate amplitude modulated signals [1]. Kamshilin *et al.* [5] showed that by summing up each frame $I(t)$ of an iPPG recording multiplied by the corresponding value of a reference function $R_C(t)$, a perfusion map S_C can be obtained:

$$S_C(x,y) = \sum_t I(x,y,t) \cdot R_C(t) \quad (1)$$

We can extract the phase map by calculating the argument of S_C . Kamshilin *et al.* [5] use a reference function that attempts to take the HRV into account. The reference function is formed by spatially averaging all pixel traces of I . Then, Fourier transform is applied to the iPPG signal. From the resulting power spectrum, we select a narrow frequency band around the heart rate. Using not a single frequency but a frequency band introduces temporal variability in the reference function (HRV). We then apply inverse Fourier transform to the selected band and obtain the complex reference function $R_C(t)$. [5]

Method 2: Zaunseder *et al.* used in [16] a simplified approach just relying on a single frequency. Thus, $R_C(t)$ consequently consists of a sine wave and a cosine wave both at heart rate and HRV is not considered. [16]

Method 3: Frassinetti *et al.* [2] suggested an alternative approach for generating phase maps in which cross-correlation of the reference function $R_C(t)$ and the pixel traces of I is used:

$$\psi(x,y,k) = \lim_{M \rightarrow \infty} \frac{1}{2M+1} \sum_{t=-M}^M R_C(t) \cdot I(x,y,t+k) \quad (2)$$

For this method, a real-valued reference function is sufficient. We altered the original approach of Frassinetti *et al.* [2] such that the reference function consists of the spatially averaged iPPG signal.

2.2.2 Spatial Assessment

For the spatial assessment of the phase maps we derived a statistical parameter (empirical standard deviation) and two textural parameters (homogeneity and contrast) from the phase maps. The calculation of the textural parameters is based on gray-level co-occurrence matrices (GLCMs) of the phase maps. A detailed explanation of textural parameters is given in the works of Haralick *et al.* [3, 4]. In short, a GLCM contains information about the frequency of gray levels in defined spatial relationships. Textural parameters can be extracted from GLCMs and describe the distribution of probabilities of certain gray level pairings. Based on the results of previous tests, we only used homogeneity and contrast for our analysis. In our implementation we used a symmetric counting method of gray level pairings. Furthermore we considered all four principal directions, thus obtaining four GLCMs. We then combined these four matrices in order to include all directions in

our calculation. Two distances (1 and 4) between the pixel of interest and its neighbours were examined. We used two ways to handle grayscale values. In one method no restrictions were made, in the other method the gray levels were restricted to a range between the 10th and 90th percentile of the average of all phase maps of the respective data set. Values outside such percentiles were considered as outliers and not counted. Overall, four GLCMs per phase map were assessed (two distances, with/without restrictions). The two considered textural parameters were then used to evaluate the GLCMs.

2.2.3 Statistical Assessment

We conducted a Friedman test over all analysis intervals in order to statistically assess if differences upon stimuli occur at any of the spatial measures. As post-hoc test, we applied the Wilcoxon test. Post-hoc tests were only carried out between analysis intervals where we expected a difference caused by a stimulus. Hence, we compared the intervals before and after a CFT against each other. We did not use any correction of the significance level for the CFT study, due to the fact that the examined contrasts are orthogonal. This is not the case for CPT study. There we considered three factor levels. Thus, we applied the Bonferroni correction and adjusted the significance level to $\frac{\alpha}{3}$ with $\alpha = 0.05$ being the original significance level.

3 Results

The results of the CPT study show barely any significant changes between the considered intervals. Also, no plausible trends can be observed. The CFT study exhibits significant results for the standard deviation and some parameterizations of the textural parameters. The data also shows several trends: standard deviation and contrast increase upon stimulus, whereas homogeneity decreases. While the considered algorithms have the overall trends in common, quantitative results differ clearly. The results of the Wilcoxon test are listed in Tab. 1. Across all participants we found a correlation of $r = 0.82 \pm 0.23$ (CFT) and $r = 0.76 \pm 0.27$ (CPT) between phase maps from method 1 and 2, $r = 0.80 \pm 0.14$ (CFT) and $r = 0.81 \pm 0.16$ (CPT) for method 1 and 3 and $r = 0.66 \pm 0.24$ (CFT) and $r = 0.65 \pm 0.28$ (CPT) for method 2 and 3.

4 Discussion

We assume both stimuli to induce cutaneous vasoconstriction in the recording area. For CFT, local vasoconstriction prevents

Tab. 1: Results of the Wilcoxon test for the CFT study. Represented are the p values (* $p < 0.05$, ** $p < 0.01$). The parentheses behind the textural parameters contain a number that specifies the distance used to obtain the respective GLCM. An additional 'restr.' states, whether gray levels were restricted. 'n.t.' epitomizes 'not tested'. Green color marks an increase of the median by 10%, red the contrary.

Parameter		Zaunseder	Kamshilin	Frassinetti
Standard dev.	CFT1	0.0067**	0.0479*	n.t.
Standard dev.	CFT2	0.1688	0.7197	n.t.
Standard dev.	CFT3	0.1514	0.1876	n.t.
Hom. (1)	CFT1	n.t.	n.t.	n.t.
Hom. (1)	CFT2	n.t.	n.t.	n.t.
Hom. (1)	CFT3	n.t.	n.t.	n.t.
Hom. (4)	CFT1	n.t.	n.t.	n.t.
Hom. (4)	CFT2	n.t.	n.t.	n.t.
Hom. (4)	CFT3	n.t.	n.t.	n.t.
Cont. (1)	CFT1	0.0413*	0.2769	n.t.
Cont. (1)	CFT2	0.0067**	0.6788	n.t.
Cont. (1)	CFT3	0.2524	0.0020**	n.t.
Cont. (4)	CFT1	0.0256*	0.1205	n.t.
Cont. (4)	CFT2	0.0054**	0.7615	n.t.
Cont. (4)	CFT3	0.2078	0.0034**	n.t.
Hom. (1, restr.)	CFT1	0.0151*	0.1876	0.0946
Hom. (1, restr.)	CFT2	0.4543	0.9341	0.3028
Hom. (1, restr.)	CFT3	0.0301*	0.0413*	0.8469
Hom. (4, restr.)	CFT1	0.0302*	0.0103*	0.0034**
Hom. (4, restr.)	CFT2	0.1688	1.0000	0.0479*
Hom. (4, restr.)	CFT3	0.0125*	0.0353*	0.9341
Cont. (1, restr.)	CFT1	0.0353*	0.1514	0.1070
Cont. (1, restr.)	CFT2	0.0730	0.9341	0.4887
Cont. (1, restr.)	CFT3	0.0256*	0.1205	0.6788
Cont. (4, restr.)	CFT1	0.0256*	0.0833	0.0637
Cont. (4, restr.)	CFT2	0.0946	0.9780	0.4543
Cont. (4, restr.)	CFT3	0.0637	0.2293	0.7615

blood from circulating through peripheral vessels. CPT causes a cold pain at the application site, which triggers sympathetic response and vasoconstriction. [8]

Because of the vascular structure, phase maps incorporate a certain degree of inhomogeneity. Vasoconstriction is likely to amplify the inhomogeneity due to the contracting vessels increasing the distance between themselves. Also, locally different vasoconstriction causes varying delays of the pulsation, thus amplifying the inhomogeneity as well [2]. In the GLCM, homogeneity indicates small gray level differences in the geometrical structure, whereas standard deviation and contrast are measures for a high dispersion. Hence, we expect homogeneity to decrease upon stimulus and the latter parameters to increase.

Concerning CFT, all considered methods show the expected trends to some extent. Method 2 matches the expected physiological reaction most closely as indicated by the found trends. Additionally, the method provides the highest number of sig-

nificant p values, thus demonstrating the effect of the stimuli more clearly than the other methods.

The results of the CPT study are more ambiguous than those of the CFT study. This could be due to the fact, that in the CPT study the location of stimulation and the ROI do not coincide, whereby the effect of the stimulus is attenuated. We further have to consider, however, that the validation in this work is solely based on our expectation concerning the physiological reaction. Although the literature supports this expectation, there is no metrological prove and interacting physiological mechanisms might interfere with the true reaction.

The different results for the three considered algorithms stem from different calculation methods. Method 3 could be more susceptible to noise than the approaches that use synchronous detection. So the low signal-to-noise ratio of iPPG recordings could explain why this method is less sensitive to the cold stimuli than the other methods. Method 1 has a systematic error produced by using synchronous detection with a frequency band. The method yields a reference function, that consists of a sum of sine and cosine waves. This produces several error terms, that distort the estimation of the time delay. The problem of discarding HRV, which is a drawback of method 2, might not become relevant as the time intervals only last 10 s.

5 Conclusion

Our work shows the different maps to reflect our expectation in varying degrees. We cannot make propositions regarding absolute errors of the phase maps. The absolute values of phase maps are important in order to exploit temporal differences in iPPG signals. In future works, methods for the generation of phase maps should be compared quantitatively by means of model data and existing methods should be refined to be able to reveal subtle changes.

Author Statement

Research funding: Funded by the Deutsche Forschungsgemeinschaft (DFG, German Research Foundation) - 401786308. Conflict of interest: Authors state no conflict of interest. Informed consent: Informed consent has been obtained from all individuals included in this study. Ethical approval: The research related to human use complies with all the relevant national regulations, institutional policies and was performed in accordance with the tenets of the Helsinki Declaration, and has been approved by the institutional review board of the TU Dresden (EK168052013 and EK119032016).

References

- [1] M. P. Fitz. *Fundamentals of Communication Systems*. Number 1. McGraw-Hill, 2007.
- [2] L. Frassinetti, F. Giardini, A. Perrella, M. Sorelli, L. Sacconi, and L. Bocchi. Evaluation of spatial distribution of skin blood flow using optical imaging. In A. Badnjevic, editor, *Proceedings of the International Conference on Medical and Biological Engineering 2017*, volume 62, pages 74–80. Springer, 2017.
- [3] R. M. Haralick. Statistical and structural approaches to texture. 67(5):786–804, 1979.
- [4] R. M. Haralick, K. Shanmugam, and I. Dinstein. Textural Features for Image Classification. *IEEE Transactions on Systems, Man and Cybernetics*, SMC-3(6):610 – 621, 1973.
- [5] A. A. Kamshilin, S. Miridonov, V. Teplov, R. Saarenheimo, and E. Nippolainen. Photoplethysmographic imaging of high spatial resolution. *Biomedical Optics Express*, 2(4):996 – 1006, 2011.
- [6] A. Moço, S. Stuijk, M. Van Gastel, and G. De Haan. Impairing Factors in Remote-PPG Pulse Transit Time Measurements on the Face. pages 1439–1447, 2018.
- [7] A. V. Moço, S. Stuijk, and G. de Haan. Skin inhomogeneity as a source of error in remote PPG-imaging. *Biomedical Optics Express*, 7(11):4718 –4733, 2016.
- [8] H.-C. Pape, A. Kurtz, and S. Silbernagl. *Physiologie*. Georg Thieme Verlag, 2018.
- [9] V. Teplov. *Blood Pulsation Imaging*. Dissertation, University of Eastern Finland, 2014.
- [10] V. Teplov, E. Nippolainen, and A. A. Kamshilin. Optical system for monitoring dynamics of blood perfusion. *AIP Conference Proceedings*, 1537(1):218–225, 2013.
- [11] V. Teplov, E. Nippolainen, A. A. Makarenko, R. Giniatullin, and A. A. Kamshilin. Ambiguity of mapping the relative phase of blood pulsations. *Biomedical Optics Express*, 5(9):3123, 2014.
- [12] V. Teplov, A. Shatillo, E. Nippolainen, O. Gröhn, R. Giniatullin, and A. A. Kamshilin. Fast vascular component of cortical spreading depression revealed in rats by blood pulsation imaging. *Journal of Biomedical Optics*, 19(4):046011, 2014.
- [13] W. Verkrusse, L. O. Svaasand, and J. Nelson. Remote plethysmographic imaging using ambient light. *Optics Express*, 16(26):21434–21445, 2008.
- [14] J. Yang, B. Guthier, and A. E. Saddik. Estimating Two-Dimensional Blood Flow Velocities From Videos. *International Conference on Image Processing (ICIP)*, pages 3768–3772, 2015.
- [15] N. Zaproudina, V. Teplov, E. Nippolainen, J. A. Lipponen, A. A. Kamshilin, M. Närhi, P. A. Karjalainen, and R. Giniatullin. Asynchronicity of facial blood perfusion in migraine. *PLoS ONE*, 8(12), 2013.
- [16] S. Zauneder, A. Trumpp, H. Ernst, M. Förster, and H. Malberg. Spatio-temporal analysis of blood perfusion by imaging photoplethysmography. *Optical Diagnostics and Sensing XVIII: Toward Point-of-Care Diagnostics*, 10501(February):15, 2018.